

Layer-by-Layer Self-Assembled Osmium Polymer-Mediated Laccase Oxygen Cathodes for Biofuel Cells: The Role of Hydrogen Peroxide

Pablo Scodeller,[†] Romina Carballo,[†] Rafael Szamocki,^{†,§} Laura Levin,[‡]
Flavia Forchiassin,[‡] and Ernesto J. Calvo^{*,†,§}

INQUIMAE-DQIAyQF, Facultad de Ciencias Exactas y Naturales, Universidad de Buenos Aires, 1428 Buenos Aires, Argentina, Micología Experimental, Departamento de Biodiversidad y Biología Experimental, Facultad de Ciencias Exactas y Naturales, Universidad de Buenos Aires, 1428 Buenos Aires, Argentina, and Saarland University, 66123 Saarbrücken, Germany

Received March 17, 2010; E-mail: calvo@qi.fcen.uba.ar

Abstract: High potential purified *Trametes trogii* laccase has been studied as a biocatalyst for oxygen cathodes composed of layer-by-layer self-assembled thin films by sequential immersion of mercaptopropene sulfonate-modified Au electrode surfaces in solutions containing laccase and osmium-complex bound to poly(allylamine), (PAH–Os). The polycation backbone carries the Os redox relay, and the polyanion is the enzyme adsorbed from a solution of a suitable pH so that the protein carries a net negative charge. Enzyme thin films were characterized by quartz crystal microbalance, ellipsometry, cyclic voltammetry, and oxygen reduction electrocatalysis under variable oxygen partial pressures with a rotating disk electrode. New kinetic evidence relevant to biofuel cells is presented on the detection of traces of H₂O₂, intermediate in the O₂ reduction, with scanning electrochemical microscopy (SECM). Furthermore the inhibitory effect of peroxide on the biocatalytic current resulted in abnormal current dependence on the O₂ partial pressure and peak shape with hysteresis in the polarization curves under stagnant conditions, which is offset upon stirring with the RDE. The new kinetic evidence reported in the present work is very relevant for the operation of biofuel cells under stagnant conditions of O₂ mass transport.

1. Introduction

Efficient energy conversion in a biofuel cell requires that the enzyme-modified electrode exhibit fast kinetics for the reaction of the enzyme with its substrate at low overpotential. According to the Marcus theory, the rate of the enzyme–mediator reaction depends on the reorganization energy and the free energy driving force, i.e. the difference between the enzyme active-site redox potential and the mediator electrochemical potential.¹ The kinetics of an amperometric enzyme electrode such as an O₂ biocathode for a biofuel cell are also determined by the interplay of enzyme–mediator and enzyme–oxygen kinetics and redox charge diffusion.²

The multicopper enzyme laccase (EC1.10.3.2; benzenediol: oxygen oxidoreductase) is an extracellular blue copper enzyme in plants and fungi which catalyzes the oxidation of biphenols and the four-electron reduction of molecular oxygen to water. It contains four copper atoms, denoted T1, T2, and two T3 according to their spectroscopic properties. In high potential laccases the copper center T1 can be reduced by phenol compounds, one-electron redox mediators, and direct electron transfer from electrodes. While substrates are oxidized at the

T1 copper site, further internal electron transfer leads to the reduction of molecular O₂ at the trinuclear T2/T3 cluster.^{3–5}

The catalytic ability of laccases to activate the four-electron reduction of oxygen under physiological conditions at unprecedented high electrode potentials (between 0.35 V and 0.50 V vs Ag/AgCl) has encouraged their study in cathodes for biofuel cells, and an extensive literature on the electrochemistry of laccases from different sources has followed in recent years.^{6–9} Note, however, that the results from physiological conditions have been extrapolated to electrochemical-mediated conditions without further proof.

In the present communication we extend the previous work with *Trametes trogii* laccase¹⁰ (Lac) self-assembled layer by layer (LbL) by sequential electrostatic adsorption of PAH–Os

- (3) Shleev, S.; Tkac, J.; Christenson, A.; Ruzgas, T.; Yaropolov, A. I.; Whittaker, J. W.; Gorton, L. *Biosens. Bioelectron.* **2005**, *20* (12), 2517–2554.
- (4) Solomon, E. I.; Baldwin, M. J.; Lowery, M. D. *Chem. Rev.* **1992**, *92* (4), 521–542.
- (5) Solomon, E. I.; Sundaram, U. M.; Machonkin, T. E. *Chem. Rev.* **1996**, *96* (7), 2563–2605.
- (6) Tarasevich, M. R.; Bogdanovskaya, V. A.; Kuznetsova, L. N. *Russ. J. Electrochem.* **2001**, *37* (8), 833–837.
- (7) Palmore, G. T. R.; Kim, H. H. *J. Electroanal. Chem.* **1999**, *464* (1), 110–117.
- (8) Chen, T.; Barton, S. C.; Binyamin, G.; Gao, Z. Q.; Zhang, Y. C.; Kim, H. H.; Heller, A. *J. Am. Chem. Soc.* **2001**, *123* (35), 8630–8631.
- (9) Calabrese Barton, S.; Kim, H. H.; Binyamin, G.; Zhang, Y.; Heller, A. *J. Am. Chem. Soc.* **2001**, *123* (24), 5802–3.

[†] INQUIMAE-DQIAyQF.

[‡] Micología Experimental.

[§] Saarland University.

(1) Mano, N.; Soukharev, V.; Heller, A. *J. Phys. Chem. B* **2006**, *110* (23), 11180–11187.

(2) Bartlett, P. N. *Bioelectrochemistry. Fundamentals, Experimental Techniques and Applications*; John Wiley & Sons: Chichester, 2008.

and Lac on mercaptopropyl sulfonate (MPS) thiolated gold surfaces. A recent report of Lvov¹¹ described the LbL of laccase with (non-redox) poly(dimethylammonium chloride) multilayers on cellulose microfibrillar surfaces to fabricate bioactive composites. Lisdat et al. have recently reported the LbL self-assembly of Lac and cytochrome *c* as electron carrier and redox mediator.^{12,13}

In order to achieve reproducible enzyme electrodes, it is essential to control the film thickness, the enzyme and mediator surface loading, the variation of oxygen partial pressure, convective-diffusion mass transport in the liquid electrolyte, and control of the topmost layer charge, etc.^{2,14} This can be achieved by using the LbL electrostatic adsorption technique pioneered by Decher.¹⁵ The advantage of the LbL self-assembly over hydrogels of the same composition is that the electrodes can be designed and built choosing from different variables such as thickness, enzyme loading, osmium concentration, and charge of the topmost layer. Several rate-determining steps can be identified in the overall process: (i) enzyme–substrate kinetics, (ii) enzyme–cosubstrate (redox mediator), (iii) partition and mass transport of substrate in the enzyme layer, (iv) concentration of redox mediator in the film and rate of electron propagation through the enzyme layer, and (v) mass transport of the enzyme substrate (oxygen) in the solution adjacent to the enzyme layer on the electrode surface.

Herein, we report important new kinetic evidence for the biocatalytic cathodic reduction of O₂ mediated by an osmium-based polymer relay:

the detection of peroxide by SECM,

its inhibitory effect on the biocathode under stagnant conditions, and

the offset of the inhibition upon stirring with the RDE. Also, we present the effect of film thickness on the O₂ biocatalysis and the inhibition of the biocathode.

2. Experimental Section

2.1. Reagents. **2.1.1. Organism.** Purified enzyme laccase from *Trametes trogii* has been employed in this study.¹⁶ Strain 463 (BAFC: Mycological Culture Collection of the Department of Biological Sciences, Faculty of Exact and Natural Sciences, University of Buenos Aires) of *Trametes trogii* (*Funalia trogii*) (*Polyporaceae*, *Aphylliphorales*, *Basidiomycetes*) was used in these experiments. Stock cultures were maintained on malt extract agar slants at 4 °C.

2.1.2. Culture Conditions. Medium for fungal culture (GA medium) contained glucose, 20 g; MgSO₄·7H₂O, 0.5 g; KH₂PO₄, 0.5 g; K₂HPO₄, 0.6 g; MnCl₂·4H₂O, 0.09 mg; H₃BO₃, 0.07 mg; Na₂MoO₄·H₂O, 0.02 mg; FeCl₃, 1 mg; ZnCl₂, 3.5 mg; thiamine hydrochloride, 0.1 mg; asparagine monohydrate, 3 g; distilled water up to 1 L, supplemented with 1 mM copper sulfate. Initial pH of the medium was adjusted to 6.5 with NaOH 1 N. Erlenmeyer flasks (500 mL size) with 50 mL of medium were inoculated with four 25-mm² surface agar plugs from a 7-day-old culture grown on malt

agar (1.3% malt extract, 1% glucose, agar 2%). Incubation was carried out statically at 28 ± 1 °C. Cultures were harvested at day 22 and filtered through a filter paper using a Büchner funnel; the culture supernatants were used as enzyme sources.

MALDI-TOF mass spectra were acquired with a Omnixflex Bruker Daltonics mass spectrometer operated in the linear mode at an accelerating voltage of 19 keV. α -Cyano-4-hydroxycinnamic acid was used as a matrix. The molecular masses of both laccase proteins were 56 kDa from *Trametes trogii* and 59 kDa from *Trametes versicolor* (see Supporting Information).

2.1.3. Enzyme Purification.

2.1.3.1. Filtration and Precipitation of Proteins. The crude yellow solution from culture was filtered through filter paper. The proteins were then precipitated by slow stirring in an ice bath and adding slowly (NH₄)₂SO₄ until saturation. After 1 h when the proteins precipitated completely, the solution was centrifuged in a Beckmann centrifuge (30 min, 5500 rpm, 17-in. rotor).

The pellet was dissolved in 20 mM Tris buffer of pH 7.0, and 3-mL portions were eluted in a series of 2 Hitrap (GE Healthcare) desalting columns, collecting fractions with absorption at 280 nm which were further dialyzed and freeze-dried.

2.1.3.2. FPLC. Ion-Exchange Chromatography and Size Exclusion Chromatography. The crude dried protein sample was dissolved in 0.1 M Tris buffer of pH 6 (100 mg·mL⁻¹). This enzyme preparation was fed into an ion-exchange HiPrep 16/10 Q FF (Amersham Bioscience) column in portions of 500 μ L and equilibrated with the same buffer at a flow rate of 4 mL·min⁻¹. The retained proteins were eluted using the following NaCl gradient: 0 to 300 mM, 15 min; 300 mM, 5 min; 300 mM to 1 M, 3 min; and 300 mM, 15 min. A first fraction with laccase activity was pooled, dialyzed against Milli-Q water, and lyophilized. The second fraction was not active with ABTS and contained the yellow pigment (see Supporting Information).

Portions of 10 mg of the resulting powder laccase from the first column were dissolved in 250 μ L of 0.1 M acetate buffer (pH 4.7), centrifuged at 10,000g in order to remove solid compounds, and applied to a size-exclusion Superdex 200 10/300 GL column (Amersham Bioscience) with 0.1 M acetate buffer, pH 4.7, at a flow rate of 0.5 mL·min⁻¹. This column yielded three peaks, the first of which was ABTS laccase active that was pooled, dialyzed against Milli-Q water, and lyophilized. The absorption ratio A₆₁₀/A₂₈₀ increased 4-fold as the crude enzyme was purified.

For details of chromatograms and characterization of the purified enzymes see Supporting Information.

2.1.4. Enzyme Activity. Enzyme activity was measured spectrophotometrically in sodium acetate buffer pH 5 at 25 °C using 2,2'-azinobis-3-ethylbenzothiazoline-6-sulfonate (ABTS).⁴² Oxidation of ABTS was determined by the increase in A₄₂₀ (ϵ_{420} = 36 mol·cm⁻¹·mL). Laccase activity has been expressed in International Units (U), as the amount of enzyme needed to release 1 μ mol of product per min. The activity of the crude enzyme solution was determined to be 650 U·mg⁻¹, while the purified enzyme had an activity of 134 U·mg⁻¹.

2.1.5. Chemicals. 3-Mercaptopropyl sulfonate (MPS), potassium nitrate, Na₂HPO₄, and NaH₂PO₄ were purchased from Sigma. 2,2'-azinobis-3-ethylbenzothiazoline-6-sulfonate (ABTS), poly(allylamine) (PAH), poly(sodium vinyl sulfonate) (PVS), sodium acetate, and acetic acid (100%) were from Fluka. All reagents were analytical grade and used without further purification except PAH which were dialyzed against Milli-Q water. Ultrapure water was obtained from a Milli-Q purification system (nominal resistivity 18.2 M Ω at 25 °C) and used to prepare all solutions.

The complex [Os(bpy)₂Cl(PyCOH)]Cl (where PyCOH is pyridine carbaldehyde, in this article called "Os complex") and osmium poly(allylamine) (PAH–Os) were synthesized as described elsewhere.¹⁷ This polymer solution was purified by dialysis against

(10) Szamocki, R.; Flexer, V.; Levin, L.; Forchiassin, F.; Calvo, E. J. *Electrochim. Acta* **2009**, *54* (7), 1970–1977.

(11) Xing, Q.; Eadula, S. R.; Lvov, Y. M. *Biomacromolecules* **2007**, *8* (6), 1987–1991.

(12) Lisdat, F.; Dronov, R.; Mohwald, H.; Scheller, F. W.; Kurth, D. G. *Chem. Commun.* **2009**, (3), 274–283.

(13) Balkenhohl, T.; Adelt, S.; Dronov, R.; Lisdat, F. *Electrochem. Commun.* **2008**, *10* (6), 914–917.

(14) Flexer, V.; Pratt, K. F. E.; Garay, F.; Bartlett, P. N.; Calvo, E. J. *J. Electroanal. Chem.* **2008**, *616* (1–2), 87–98.

(15) Decher, G. *Science* **1997**, *277* (5330), 1232–1237.

(16) Levin, L.; Forchiassin, F.; Viale, A. *Process Biochem.* **2005**, *40* (3–4), 1381–1387.

(17) Danilowicz, C.; Corton, E.; Battaglini, F. *J. Electroanal. Chem.* **1998**, *445* (1–2), 89–94.

Table 1. Details of Concentrations of Enzyme Film Multilayers

| layers | QCM $\mu\text{g} \cdot \text{cm}^{-2}$ | Γ_{enz} $\text{mol} \cdot \text{cm}^{-2}$ | Q $\mu\text{C} \cdot \text{cm}^{-2}$ | Γ_{Os} $\text{mol} \cdot \text{cm}^{-2}$ | d nm | [Lac] mM | [Os] mM |
|--------|--|---|--|--|--------|----------|---------|
| 1 | 1.05 | 1.91×10^{-11} | 0.58 | 6×10^{-12} | 4.2 | 45 | 71.5 |
| 3 | 2.23 | 4.05×10^{-11} | 1.26 | 1.3×10^{-11} | 8.4 | 48 | 77.0 |
| 6 | 5.20 | 9.45×10^{-11} | 1.74 | 1.8×10^{-11} | 17.9 | 53 | 50.0 |

water for 3 days. The osmium content was evaluated spectrophotometrically at $\lambda = 475$ nm ($\epsilon = 8100 \text{ M}^{-1} \cdot \text{cm}^{-1}$). Soluble $[\text{Os}(\text{bpy})_2\text{Cl}(\text{PyCOOH})]^+$ was prepared as described elsewhere.¹⁸

2.1.6. Layer-by-Layer Self-Assembly. The gold electrodes were polished and cleaned. Then in a first step a monolayer of MPS was formed by immersing the electrodes in a solution of 0.02 M MPS in 0.01 M H_2SO_4 for 30 min. After rinsing the electrodes with Milli-Q water, 100 μL of a solution of 0.44 mM PAH–Os of pH 8 was deposited on the electrode surface and allowed to assemble for 10 min. After rinsing, 100 μL of 134 units $\cdot \text{mL}^{-1}$ Lac in water was dropped on the same electrode, and after 10 min of self-assembly the laccase solution was removed, and the modified gold disk was rinsed with Milli-Q water. These deposition steps were repeated until the desired number of polymer and enzyme layers were deposited. In every case we covered the LbL self-assembled electrode structures with a topmost layer of PAH–Os.

2.1.7. Electrochemistry. Cyclic voltammetry was performed using an Autolab PGSTAT 30 potentiostat in a three-electrode cell with a platinum gauze as counter electrode and $\text{Ag}/\text{AgCl}/(\text{Cl } 3\text{M})$ as reference electrode (all potentials herein are referred to this reference electrode). The working electrodes were gold discs ($d = 5$ mm) embedded in Kelf polymer. All measurements were performed in 0.1 M acetate buffer of pH 4.7 containing 0.2 M KNO_3 .

Before measurements all solutions were degassed with pure argon or saturated with gas mixtures of argon/oxygen in different ratios. In order to control the oxygen partial pressure, the argon/oxygen ratio of this gas mixture was controlled by means of precision flow meters and flow regulators (G. Bruno Schilling, Argentina). Calibration of the O_2/Ar gas mixtures was performed with the rotating disk electrode (RDE) convective-diffusion limiting current density.

Detection of H_2O_2 was performed with the scanning electrochemical microscopy (SECM) with a Pt ultra-microelectrode tip poised at 1.2 V to oxidize H_2O_2 under diffusion conditions in the generator–collection mode.^{19,20} Details of the SECM setup have been given elsewhere.²¹

3. Results and Discussion

We report on the co-immobilization of laccase and a redox polyelectrolyte mediator via layer-by-layer (LbL) electrostatic self-assembly technique. This method has extensively been employed by our group and by others to form “wired” glucose oxidase, peroxidase, etc. multilayer films using redox polyelectrolytes.^{22–26} Preliminary results of molecular dioxygen catalysis

by LbL self-assembled Lac multilayers mediated by osmium polymer have been recently reported.¹⁰

Unlike randomly oriented redox hydrogels, cast, or electropolymerized films, organized nanostructured thin films allow control over the film thickness, the enzyme loading, and the mediator concentration. In addition, the nature and surface charge of the topmost layer can be controlled at will. While one assumes homogeneous composition in the x – y plane at any normal distance z from the metal surface, there is a normal distribution of species, electrostatic potential, and vector electron transfer given by a redox concentration gradient. In the present study the films comprise alternate layers of Lac and osmium polyelectrolyte mediator with some intermixing and interpenetration of these layers contributing to a flexible wiring of the enzyme due to segmental motion.

In the work reported here, the strategy has been to modify an Au electrode surface with a functional short alkane thiol carrying anionic sulfonate terminal groups and to adsorb on top of this primer layer osmium bipyridine electron relays covalently tethered to a cationic poly-electrolyte backbone. Further adsorption of Lac from a solution of a suitable pH value (around 5) where the protein carries a net negative charge (pI (laccase from *Trametes troglia*) = 3.3,²⁷ yields an all-integrated enzyme–mediator system as previously reported for glucose oxidase.²⁸

As reported in a previous communication,¹⁰ the adsorption of Lac on the PAH–Os layers was monitored with the quartz crystal microbalance (QCM) as a function of time (see Supporting Information), obtaining on average a surface concentration of $1.34 \times 10^{-11} \text{ mol} \cdot \text{cm}^{-2}$ in each adsorption step. The thickness of the enzyme–mediator thin films thus obtained was monitored by ellipsometry at 632 nm.²⁵

Cyclic voltammetry of these electrodes in O_2 -free solutions shows only the $\text{Os}(\text{III})/\text{Os}(\text{II})$ redox couple at 0.31 V as reported before.¹⁰ The difference in electrode potential from the value for soluble osmium complex (~ 0.25 V) is due to charge regulation through Donnan potential of the multilayer film.²⁹ The integrated electrical charge at low sweep rate ($5 \text{ mV} \cdot \text{s}^{-1}$) yields an average surface concentration of redox sites, $\Gamma_{\text{Os}} = (q)/(F)(\text{mol} \cdot \text{cm}^{-2})$. Table 1 summarizes the concentration and thickness of the different electrodes studied in the present work. From the surface concentrations of redox mediator and enzyme, the volume concentrations have been estimated using the ellipsometry thickness.

Notice that the [Lac] and [Os] are of similar magnitude, unlike our previous studies with glucose oxidase where $[\text{Os}] \gg [\text{GOx}]$.^{14,28} This is due to the lower surface charge on Lac as compared to that on GOx.

In the presence of O_2 , a clear catalytic reduction wave develops as can be seen in Figure 1 for films with six laccase

- (18) Ricci, A.; Rolli, C.; Rothacher, S.; Baraldo, L.; Bonazzola, C.; Calvo, E. J.; Tognalli, N.; Fainstein, A. J. *Solid State Electrochem.* **2007**, *11* (11), 1511–1520.
 (19) Eckhard, K.; Schuhmann, W. *Electrochim. Acta* **2007**, *53* (3), 1164–1169.
 (20) Evans, S. A. G.; Brakha, K.; Billon, M.; Mailley, P.; Denuault, G. *Electrochem. Commun.* **2005**, *7* (2), 135–140.
 (21) Volker, E.; Inchauspe, C. G.; Calvo, E. J. *Electrochem. Commun.* **2006**, *8* (1), 179–183.
 (22) Hodak, J.; Etchenique, R.; Calvo, E. J.; Singhal, K.; Bartlett, P. N. *Langmuir* **1997**, *13* (10), 2708–2716.
 (23) Calvo, E. J.; Etchenique, R.; Pietrasanta, L.; Wolosiuk, A.; Danilowicz, C. *Anal. Chem.* **2001**, *73* (6), 1161–1168.
 (24) Calvo, E. J.; Battaglini, F.; Danilowicz, C.; Wolosiuk, A.; Otero, M. *Faraday Discuss.* **2000**, *116* (116), 47–65.
 (25) Forzani, E. S.; Otero, M.; Perez, M. A.; Teijelo, M. L.; Calvo, E. J. *Langmuir* **2002**, *18* (10), 4020–4029.

- (26) Calvo, E. J.; Danilowicz, C.; Wolosiuk, A. *J. Am. Chem. Soc.* **2002**, *124* (11), 2452–2453.
 (27) Colao, M. C.; Garzillo, A. M.; Buonocore, V.; Schiesser, A.; Ruzzi, M. *Appl. Microbiol. Biotechnol.* **2003**, *63* (2), 153–158.
 (28) Flexer, V.; Forzani, E. S.; Calvo, E. J. *Anal. Chem.* **2006**, *78* (2), 399–407.
 (29) Tagliacuzzi, M.; Calvo, E. J.; Szeifer, I. *Electrochim. Acta* **2008**, *53* (23), 6740–6752.

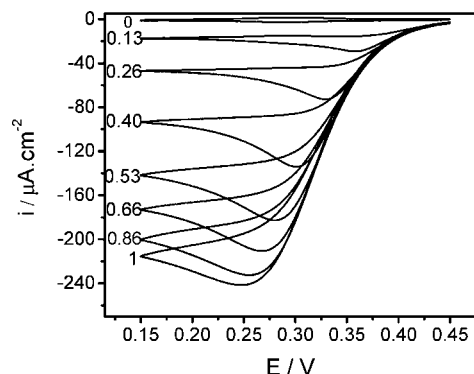


Figure 1. Cyclic voltammetry for different oxygen partial pressures under stagnant conditions for six bilayers of Laccase and PAH–Os, sweep rate $\nu = 5 \text{ mV}\cdot\text{s}^{-1}$ in 0.1 M acetate buffer of pH 4.7 and 0.2 M KNO_3 .

layers at different oxygen partial pressures. It should be noticed that for films thicker than three layers appreciable hysteresis between the forward and backward potential scans can be observed with a current maximum and diffusion tailing which indicates some mass transport limitation. The hysteresis and peak are more clearly seen the lower the oxygen partial pressure is and the thicker the enzyme–polymer films are (Figures 1 and 2).

This could arise from depletion of the oxygen concentration within the enzyme film or in the electrolyte adjacent to the enzyme electrode surface. Another feature in Figure 1 is the shift of the half wave potential to lower values, the higher the oxygen partial pressure.

Note that similar hysteresis and current maximum have been seen in previous air-saturated solution,^{10,30} but no explanation has been advanced. Notice that in a recent report, hysteresis and current peak under air-saturated solution have been shown, while a fully developed catalytic wave was apparent under oxygen saturation.³¹ In our hands this could be reproduced and offset by rotation (see Supporting Information).

3.1. Convective-Diffusion with Rotating Disc Electrode. Diffusion in the enzyme layer or in the solution adjacent to the electrode can be distinguished by control of convective-diffusion in the electrolyte solution with the rotating disk electrode. Upon stirring the external solution with a rotating disk electrode (RDE), the hysteresis disappears, and well-developed catalytic current waves reach a plateau at the most reducing potentials as shown in Figure 2 for different numbers of PAH–Os/Lac bilayers in O_2 -saturated solutions. Larger differences between stagnant and stirred solutions are apparent with thicker films.

In Figure 2 a series of O_2 reduction catalytic waves at 9 Hz show that the cathodic current increases with the electrode potential and the number of LbL layers. As the electrode potential decreases, the catalytic current follows the Os(II) concentration in the polymer layer (Nernstian dependence) and reaches a plateau at the most reducing potentials when all the osmium sites in the polymer film have been reduced ($\sim 0.1 \text{ V}$). The half wave potential $E_{1/2}$ decreases slightly for $(\text{Lac})_6(\text{PAH–Os})_7$ and is close but always positive to the formal redox potential of the osmium mediator in the film under those conditions (see below).

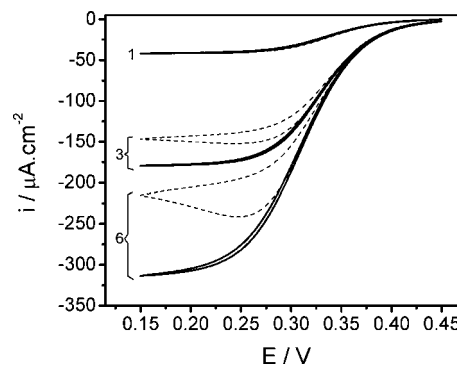


Figure 2. Cyclic voltammetry for different numbers of bilayers, at a rotation frequency of 9 Hz (solid line) and stagnant condition (dashed line) for scan rate $\nu = 5 \text{ mV}\cdot\text{s}^{-1}$ in oxygen-saturated 0.1 M acetate buffer of pH 4.7 and 0.2 M KNO_3 .

The rotating disk electrode provides well-controlled conditions for the convective-diffusion mass transport³² of reactants toward the electrode and soluble intermediates and products toward the bulk electrolyte. The convective-diffusion limiting current density for the reduction of O_2 is given by the Levich equation:³³

$$i_L = 1.55 \cdot NFD_{\text{O}_2}^{2/3} \nu^{-1/6} C_{\text{O}_2}^* f^{1/2} \quad (1)$$

where F = the Faraday constant, D_{O_2} = the oxygen diffusion coefficient ($1.41 \times 10^{-5} \text{ cm}^2\cdot\text{s}^{-1}$), ν = the kinematic viscosity of the electrolyte ($0.01 \text{ cm}^2\cdot\text{s}^{-1}$), $C_{\text{O}_2}^*$ = the analytical oxygen concentration (1 mM at $P_{\text{O}_2} = 1 \text{ atm}$), f = the rotation frequency in Hz, and N = the number of electrons transferred per oxygen molecule. At 9 Hz eq 1 yields $i_L = 2.25 \text{ mA}\cdot\text{cm}^2$ for $N = 4$, which is much larger than any values in Figure 2. Therefore, the flux of O_2 toward the electrode cannot be the limiting factor giving rise to the hysteresis and the maximum in the catalytic wave shown in Figures 1 and 2. The catalytic current is always less than the convective-diffusion limiting current and increases with the number of enzyme layers and the lower the oxygen partial pressure (see Table 1 in Supporting Information).

Notice that the O_2 reduction reaction consumes 4 mol protons/mol oxygen. Thus, the concentration of $[\text{H}^+] = 2 \times 10^{-5} \text{ M}$ at pH 4.7, is much less than 1 mM of dissolved oxygen in the aqueous electrolyte, but the concentration of acetic acid is $[\text{AcOH}] \approx 0.05 \text{ M}$ for 0.1 M acetate buffer of pH 4.7 which can readily dissociate, yielding protons. Since the electrolyte is well buffered under these conditions, it is not expected that the diffusion of the acid form of the buffer which yields protons at the surface can limit the oxygen catalytic current.³⁴

Therefore, it can be concluded that some other soluble diffusing species should be involved, i.e. a laccase-inhibiting species accumulated in the enzyme layer and diffusing away from the enzyme multilayer electrode to the electrolyte solution driven by the rotation may be the cause of the observed hysteresis and decay under stagnant conditions.

It is well recognized that laccase reduces oxygen by a four-electron mechanism under physiological conditions with the trinuclear cluster T2/T3 as the oxygen reduction site with the

(30) Nazaruk, E.; Michota, A.; Bukowska, J.; Shleev, S.; Gorton, L.; Bilewicz, R. *J. Biol. Inorg. Chem.* **2007**, *12* (3), 335–344.

(31) Ackermann, Y.; Guschin, D. A.; Eckhard, K.; Shleev, S.; Schuhmann, W. *Electrochem. Commun.* **2010**, *12*, 640–643.

(32) Bard, A. J.; Faulkner, L. R., *Electrochemical Methods: Fundamentals and Applications*, 2nd ed.; John Wiley & Sons: New York, 2001.

(33) Albery, W. J.; Hitchman, M. L. *Ring-Disc Electrodes*; Oxford Science Research Papers; Clarendon Press Oxford: Oxford, UK, 1971.

(34) Albery, W. J. *Trans. Faraday Soc.* **1966**, (62), 522.

supply of four electrons from the Cu T1 site close to the protein surface where the oxidation of target molecules supplies the electrons.^{3,5}

In vitro, however evidence has been found for the reduction of both the T2/T3 cluster and T1 sites either by direct electron transfer from the electrode surfaces at tunneling distance^{3,35–39} or by outer sphere one-electron redox couples.^{1,40–51} It should be stressed here that there is no experimental evidence in the latter cases for a pure four-electron oxygen reduction pathway without the release of hydrogen peroxide as a two-electron intermediate. Moreover, Solomon has shown that a peroxide intermediate occurs in the 4Cu Lac center during the reaction.⁵² Therefore, hydrogen peroxide is a good candidate as a soluble intermediate in the O₂ biocathode that could inhibit the reaction, and this inhibition would be removed if the exogenous soluble peroxide accumulated at the enzyme film surface is swept away from the enzyme multilayer surface film by the convective-diffusion effect with the RDE. Furthermore, the thicker the enzyme multilayer film, the larger accumulation of peroxide under stagnant conditions would be expected. In addition, if the self-assembled enzyme multilayer construct consists of intercalated layers of laccase and soy bean peroxidase (SBP), both enzymes wired by the osmium polymer, there is no evidence of peak current and hysteresis because any peroxide formed would be further reduced by the peroxidase (see evidence in Supporting Information).

3.2. Production of Peroxide and Inhibition of Oxygen Cathode. We have employed scanning electrochemical microscopy (SECM) in the generation-collection mode^{19,20,40,43} to investigate the production of peroxide as an intermediate of the O₂ reduction catalyzed by osmium bipyridine wired Lac. In this experiment a platinum ultra-microelectrode (UME) tip poised at 1.2 V collects (oxidizes) H₂O₂ generated during oxygen reduction at

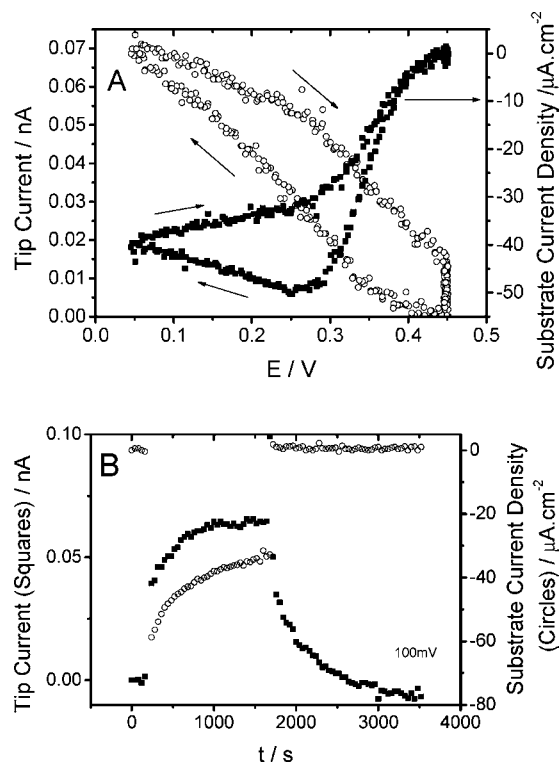


Figure 3. (A) Biocatalytic current density as a function of electrode potential for a (Lac)₆(PAH–Os)₇ in 0.1 M acetate buffer of pH 4.7 and 0.2 M KNO₃ and baseline subtracted H₂O₂ oxidation current at the tip (1.2 V) simultaneous to the substrate potential sweep at 5 mVs⁻¹. (B) Potentiostatic transient (0.45 V → 0.10 V → 0.45 V) at the Lac-modified electrode and H₂O₂ oxidation current response at the tip (1.2 V).

the Lac-modified electrode. While negligible peroxide oxidation current can be detected for the tip electrode of the SECM far from the electrode surface, H₂O₂ collection is detected upon approaching the Pt tip electrode to the oxygen biocathode. Figure 3A depicts the peroxide oxidation current at the tip as a function of the wired Lac electrode potential: H₂O₂ oxidation current increases as the O₂ reduction proceeds and also exhibits hysteresis in the reverse potential scan. Furthermore, Figure 3B shows potentiostatic transients at the Lac electrode from 0.45 V where there is no oxygen reduction, to 0.1 V where the maximum activity for the cathodic reduction is observed for the fully reduced Os(II) mediator. The H₂O₂ oxidation current at the tip follows the oxygen reduction current transient, while it decays when the electrode potential is switched back to 0.45 V.

It should be stressed that O₂ reduction does not take place on the underlying Au electrode at potentials positive to 0 V (blank experiments with redox polymer in the absence of enzyme), nor can it be reduced by Os(II).⁵³ Furthermore, in order to prove that the detected peroxide has been enzymatically produced we performed an experiment in which the addition of azide to the biocathode under steady-state operation, inhibits the enzyme and both the oxygen biocatalytic current and the SECM tip current in the collection mode for peroxide oxidation drop as shown in Figure 4. The decrease in the peroxide detection current when the biocathode is inhibited by azide (or even inactivated by chloride—data not shown) is a conclusive

- (35) Blanford, C. F.; Heath, R. S.; Armstrong, F. A. *Chem. Commun.* **2007**, (17), 1710–1712.
- (36) Pita, M.; Shleev, S.; Ruzgas, T.; Fernandez, V. M.; Yaropolov, A. I.; Gorton, L. *Electrochem. Commun.* **2006**, 8 (5), 747–753.
- (37) Ramirez, P.; Mano, N.; Andreu, R.; Ruzgas, T.; Heller, A.; Gorton, L.; Shleev, S. *Biochim. Biophys. Acta Bioenerg.* **2008**, 1777 (10), 1364–1369.
- (38) Shleev, S.; Christenson, A.; Serezhnikov, V.; Burbaev, D.; Yaropolov, A.; Gorton, L.; Ruzgas, T. *Biochem. J.* **2005**, 385, 745–754.
- (39) Shleev, S.; Jarosz-Wilkolazka, A.; Khalunina, A.; Morozova, O.; Yaropolov, A.; Ruzgas, T.; Gorton, L. *Bioelectrochemistry* **2005**, 67 (1), 115–124.
- (40) Jenkins, P. A.; Boland, S.; Kavanagh, P.; Leech, D. *Bioelectrochemistry* **2009**, 76 (1–2), 162–168.
- (41) Kavanagh, P.; Jenkins, P.; Leech, D. *Electrochem. Commun.* **2008**, 10 (7), 970–972.
- (42) Kavanagh, P.; Jenkins, P.; Leech, D. *Electrochem. Commun.* **2008**, 10 (10), 1656–1656.
- (43) Barriere, F.; Ferry, Y.; Rochefort, D.; Leech, D. *Electrochem. Commun.* **2004**, 6 (3), 237–241.
- (44) Hudak, N. S.; Gallaway, J. W.; Barton, S. C. *J. Electrochem. Soc.* **2009**, 156 (1), B9–B15.
- (45) Gallaway, J. W.; Barton, S. A. C. *J. Electroanal. Chem.* **2009**, 626 (1–2), 149–155.
- (46) Hudak, N. S.; Gallaway, J. W.; Barton, S. C. *J. Electroanal. Chem.* **2009**, 629 (1–2), 57–62.
- (47) Gallaway, J.; Wheeldon, I.; Rincon, R.; Atanassov, P.; Banta, S.; Barton, S. C. *Biosens. Bioelectron.* **2008**, 23 (8), 1229–1235.
- (48) Gallaway, J. W.; Barton, S. A. C. *J. Am. Chem. Soc.* **2008**, 130 (26), 8527–8536.
- (49) Wheeldon, I. R.; Gallaway, J. W.; Barton, S. C.; Banta, S. *Proc. Natl. Acad. Sci. U.S.A.* **2008**, 105 (40), 15275–15280.
- (50) Barton, S. C.; Pickard, M.; Vazquez-Duhalt, R.; Heller, A. *Biosens. Bioelectron.* **2002**, 17 (11–12), 1071–1074.
- (51) Farver, O.; Goldberg, M.; Wherland, S.; Pecht, I. *Proc. Natl. Acad. Sci. U.S.A.* **1978**, 75 (11), 5245–5249.
- (52) Lee, S. K.; George, S. D.; Antholine, W. E.; Hedman, B.; Hodgson, K. O.; Solomon, E. I. *J. Am. Chem. Soc.* **2002**, 124 (21), 6180–6193.

- (53) Scodeller, P.; Flexer, V.; Szamocki, R.; Calvo, E. J.; Tognalli, N.; Troiani, H.; Fainstein, A. *J. Am. Chem. Soc.* **2008**, 130 (38), 12690–12697.

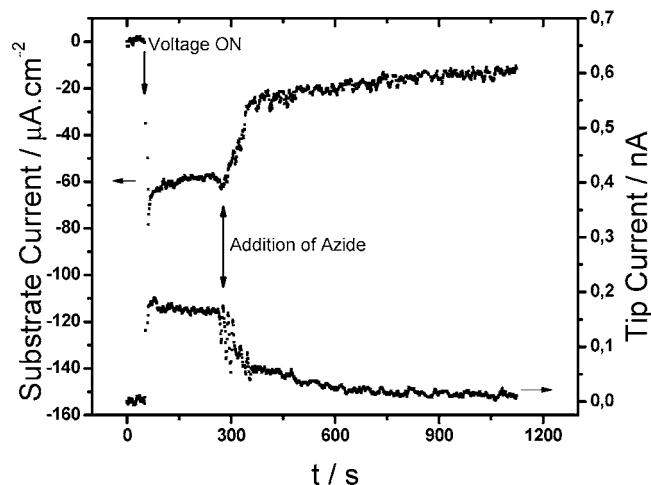


Figure 4. Effect of addition of 2 μM sodium azide to a laccase biocathode in O_2 -saturated solution of pH 5 mediated by $(\text{Lac})_3(\text{PAH-Os(II)})_4$ at 0.15 V. SECM tip potential = 1.2 V.

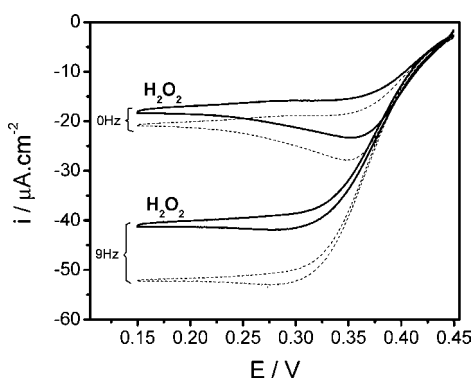


Figure 5. Effect of addition of H_2O_2 to the electrolyte on the cathodic reduction of oxygen on laccase-modified electrode $(\text{PAH-Os})_3(\text{Lac})_3(\text{PAH-Os})$ for scan rate $\nu = 5 \text{ mV} \cdot \text{s}^{-1}$ in 0.1 M acetate buffer of pH 4.7 and 0.2 M KNO_3 saturated with 0.2 atm O_2 under stagnant conditions (0 Hz) and at 9 Hz with a RDE. No peroxide (dashed line) and 100 μM peroxide (solid line).

evidence of the biocatalytic origin of hydrogen peroxide during oxygen reduction catalyzed by laccase and mediated by the Os(II) species.

Having shown that traces of peroxide are formed during the cathodic reduction of oxygen at the wired Lac cathode, we further investigated if the two-electron intermediate of the four-electron O_2 reduction inhibits the electroreduction of oxygen catalyzed by Lac and mediated by PAH–Os(II). For this, we purposely added traces of H_2O_2 (100 μM) to the electrolyte during oxygen reduction, resulting in the inhibition of the biocathode which was larger, thus increasing the exogenous peroxide concentration ($\leq 1.6 \text{ mM}$). Figure 5 depicts the resulting oxygen reduction polarization curves both in stagnant solution and under rotation at 9 Hz before and after addition of exogenous peroxide with clear decrease in the electrocatalytic O_2 reduction current.

Addition of peroxide to the solution in the absence of O_2 did not produce any cathodic current; thus, no peroxidase function has been detected for the wired Lac when exogenous peroxide is added to the external solution (see Supporting Information). This might be due to a different coordination of the exogenous peroxide to the trinuclear copper cluster as compared to the

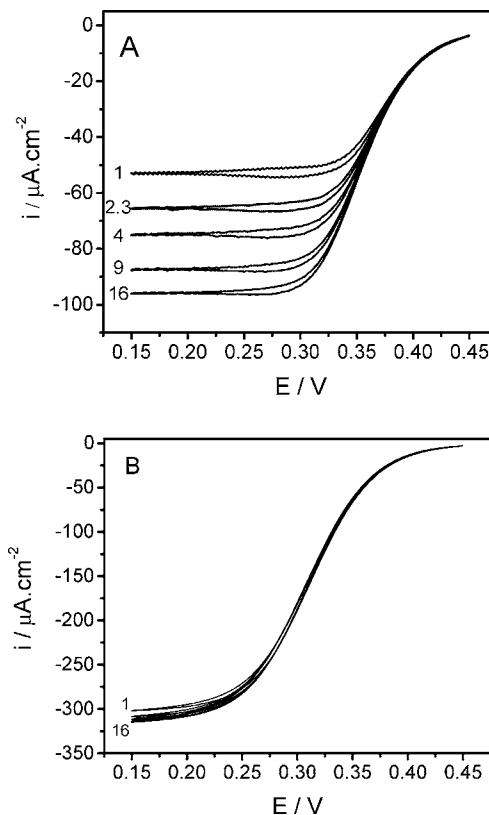


Figure 6. Polarization curves for O_2 reduction at a laccase-modified electrode $(\text{PAH-Os})_6(\text{Lac})_6(\text{PAH-Os})$ for scan rate $\nu = 5 \text{ mV} \cdot \text{s}^{-1}$ in 0.1 M acetate buffer of pH 4.7 and 0.2 M KNO_3 saturated with different oxygen partial pressures: (A) 0.13 atm O_2 ; (B) 1 atm O_2 .

peroxide intermediate in the scheme proposed by Solomon.⁵⁴ It has been reported that addition of exogenous H_2O_2 to native laccase binds to the T2 Cu^{2+} of the trinuclear cluster in the four copper atom enzyme and can replace fluoride adsorbed on that site.⁵⁵ Solomon further investigated the binding of exogenous peroxide to bridge the T2/T3 Cu centers.^{56,57}

Preliminary results in our laboratory have also shown in homogeneous solution that exogenous peroxide inhibits laccase when performed activity tests with ABTS (see evidence in Supporting Information).

3.3. Oxygen Mass Transport Effects. The effect of rotation frequency on the catalytic cathodic current is shown in Figure 6 for solutions saturated with 0.13 and 1.0 atm of oxygen, respectively. It should be noticed that the effect is stronger the lower the concentration of oxygen in the electrolyte since the enzyme-catalyzed reduction of oxygen has a complex dependence of the oxygen concentration due to the combination of Michaelis–Menten kinetics and diffusion by electron hopping in the film (see Figure 6).

Figure 6 shows clearly that at high enzyme substrate concentration Koutecky–Levich (K–L) analysis cannot be done since the current becomes independent of rotation rate due to

(54) Solomon, E. I.; Augustine, A. J.; Yoon, J. *Dalton Trans.* **2008**, (30), 3921–3932.

(55) Branden, R.; Malmström, B. G.; Vanngard, T. *Eur. J. Biochem.* **1971**, *18* (2), 238–241.

(56) Spirasolomon, D. J.; Solomon, E. I. *J. Am. Chem. Soc.* **1987**, *109* (21), 6421–6432.

(57) Palmer, A. E.; Randall, D. W.; Xu, F.; Solomon, E. I. *J. Am. Chem. Soc.* **1999**, *121* (30), 7138–7149.

the enzymatic kinetics. At low p_{O_2} also a negative shift of $E_{1/2}$ as f increases is apparent, while at high p_{O_2} no shift of $E_{1/2}$ is observed.

For mixed kinetic-diffusion control, the Koutecky–Levich equation³⁴ which describes the current density at a RDE under mixed kinetic and convective-diffusion control has been used in the case of Os polymer-mediated Lac catalysis of oxygen reduction:⁴⁸

$$\frac{1}{i} = \frac{1}{i_k} + \frac{1}{i_L} \quad (2)$$

with i_k the pure kinetic current density and $i_L = 1.55 \cdot NFD_{O_2}^{2/3} \nu^{-1/6} C^* f^{1/2}$, the convective-diffusion limiting current density. It should be borne in mind that eq 2 is strictly valid for reaction order one in the electro-active species. The oxygen concentration dependence of the cathodic O_2 reduction current density catalyzed by Lac and mediated by the osmium polymer is complex, being first order at low P_{O_2} , while a less dependent oxygen concentration current due to the Michaelis–Menten kinetics is apparent at higher P_{O_2} (see below). For electrochemical reaction order different than one, the K–L treatment leads to different equations, as shown for order 0.5 in the case of oxygen reduction on passive iron.⁵⁸ In particular, for Michaelis–Menten-type mechanisms the K–L treatment leads to the following equation:⁵⁹

$$\frac{1}{i} = \left(1 - \frac{i}{i_L}\right) \left\{ \frac{1}{NFk[Os]\Gamma_{Lac}} + \frac{1}{NFk_{cat}\Gamma_{Lac}} \right\} + \frac{K_M}{NFk_{cat}\Gamma_{Lac}C^*} + \frac{i}{i_L} \quad (3)$$

where k is the bimolecular enzyme–mediator rate constant, k_{cat} is the enzyme turnover, and K_{MS} is the Michaelis–Menten association constant for oxygen (see reaction scheme below (eq 4), Γ_{Os} and Γ_{Lac} are the surface concentrations of osmium complex and laccase.

It should be noticed that eq 3 leads to nonlinear $1/i$ vs $1/f^{1/2}$ plots due to the enzyme kinetic terms since at high oxygen concentration the current is less sensitive to the oxygen concentration. At low substrate concentration, however, for $C^* \ll K_{MS}$, a linear K–L plot can be approximated, with $(1)/(i_k) = (1)/(NFk[Os]\Gamma_{Lac}) + (1)/(NFk_{cat}\Gamma_{Lac}) + (K_M)/(NFk_{cat}\Gamma_{Lac}C^*)$ which is strictly valid for $i \ll i_L$:

$$\frac{1}{i} \approx \frac{1}{NFk[Os]\Gamma_{Lac}} + \frac{1}{NFk_{cat}\Gamma_{Lac}} + \frac{K_M}{NFk_{cat}\Gamma_{Lac}C^*} + \frac{i}{i_L} \quad (4)$$

Therefore, in the present work eq 2 (4) has been employed to extrapolate the observed current densities at $f \rightarrow \infty$ at low oxygen concentration, and the results are compiled in Figure 7 with linear Koutecky–Levich plots for six laccase layers at different oxygen partial pressure. These linear plots have variable slopes, depending on the oxygen concentration. The slope of Koutecky–Levich plots is determined by the product of three parameters, the net number of electrons transferred per reactant oxygen molecule, N , the oxygen diffusion coefficient D_{O_2} , and the analytical concentration of oxygen, C_{O_2} . At the

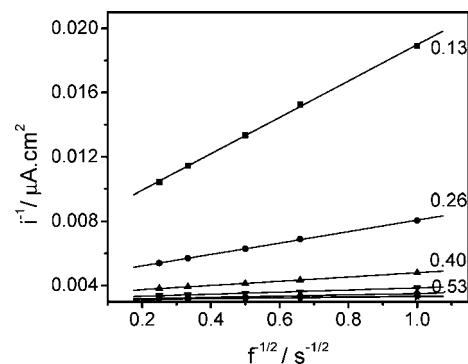


Figure 7. Koutecky–Levich plots for six laccase layers of O_2 reduction at different oxygen partial pressure. $E = 0.15$ V.

lowest oxygen concentration, $p_{O_2} = 0.13$, for $N = 4$ the expected slope is $0.0102 \mu A^{-1} \cdot cm^2 \cdot s^{1/2}$, while the experimental value is $0.0113 \mu A^{-1} \cdot cm^2 \cdot s^{1/2}$ which would yield $N = 3.62$. At higher oxygen concentrations the discrepancy between the calculated K–L slope and the extrapolated experimental current density at $f \rightarrow \infty$, $i(\infty)$ increases as shown in the Table 2 in Supporting Information.

In similar experiments Gallaway et al.⁴⁸ have reported a factor of 2 discrepancy between the calculated and the experimental K–L slopes and attributed this difference to nonunity partitioning of oxygen into the film. This would unlikely explain the difference, since in the K–L slope the oxygen concentration and diffusion coefficient are properties of the solution and not of the surface layer which would otherwise affect the intercept of K–L plots.

Since these are the most exhaustive investigations of the oxygen reduction catalyzed by laccase and mediated by osmium complexes with the RDE, we conclude that there is no clear evidence to rule out the formation and release of hydrogen peroxide under electrochemical conditions mediated by osmium complexes with $N < 4$. The kinetics in the electrochemical experiment may differ from those under physiological conditions where it has been well established that a four-electron reduction to water takes place with Lac, although peroxide has been shown to be an intermediate of the reaction which is not released into solution before four electrons and four protons are transferred to the oxygen molecule.⁵⁴

3.4. Oxygen Partial Pressure Dependence. The catalytic current for the cathodic reduction of oxygen was measured by varying the oxygen partial pressure by combination of oxygen and argon gas under control of two flow meters, with presaturation of the working solution and bubbling in the electrochemical cell while keeping the selected gas atmosphere above the electrolyte during measuring.⁵⁸ As shown in our previous communication¹⁰ an abnormal behavior in the current-concentration curve is observed, i.e. non Michaelis–Menten type behavior can be seen in Figure 8 for stagnant electrolyte: At low oxygen concentration, the curve shows an abnormal sigmoid behavior with current densities below the expected Michaelis–Menten dependence, resembling an allosteric behavior.¹⁰ The abnormal calibration curve results more evident the higher the number of assembled Lac layers. In our hands, the same behavior has been found with *Trametes versicolor* laccase from Fluka (see Supporting Information).

For osmium-mediated Lac electrodes, O_2 concentration studies are scarce in the literature with the exception of the work reported by Calabrese-Barton for data corrected by

(58) Calvo, E. J.; Schiffrin, D. J. *J. Electroanal. Chem.* **1988**, *243* (1), 171–185.

(59) Lyons, M. E. G.; Lyons, C. H.; Michas, A.; Bartlett, P. N. *J. Electroanal. Chem.* **1993**, *351* (1–2), 245–258.

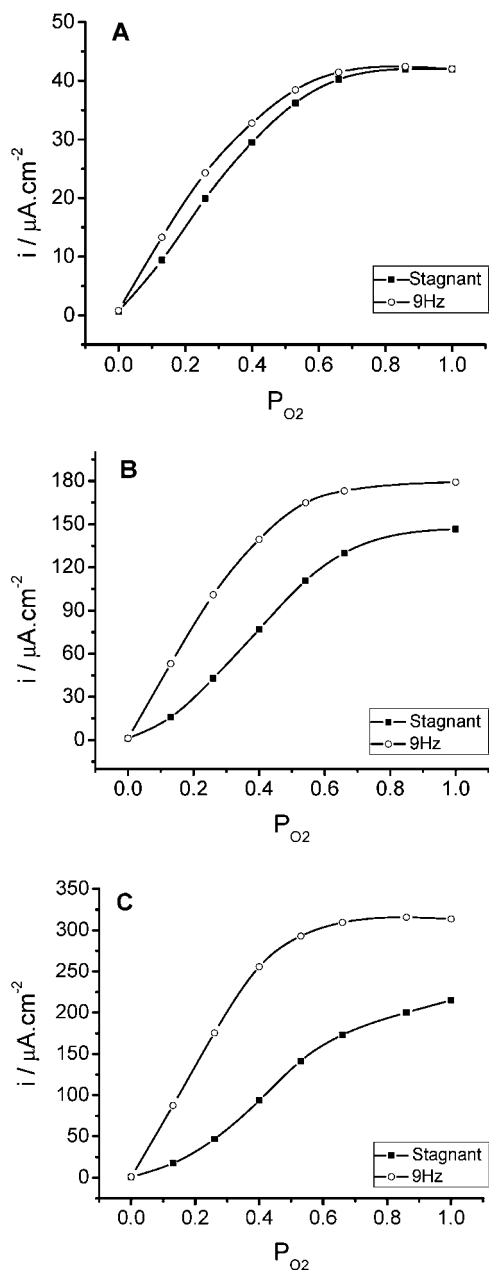


Figure 8. Catalytic current density for the electroreduction of O_2 on a laccase film mediated by PAH–Os(II) ($\text{PAH–Os}_6\text{Lac}_6(\text{PAH–Os})$) in 0.1 M acetate buffer of pH 4.7 in 0.2 M KNO_3 at different oxygen partial pressures under stagnant conditions (squares) and under rotation at 9 Hz (circles) for one bilayer (A), three bilayers (B), and six bilayers (C).

Koutecký–Levich treatment with the rotating disk electrode.⁴⁸ However, these authors did not compare their RDE results with stagnant solution, and therefore the sigmoid curve could not be observed.

Under rotation with RDE, however, larger currents are observed as explained before, and a Michaelis–Menten type behavior is apparent. The discrepancy between the oxygen reduction current density under rotation and under stagnant conditions is maximum at $P_{\text{O}_2} \approx 0.35\text{--}0.40$.

This result is consistent with the offset of the hysteresis in Figure 2 upon stirring with the RDE and the inhibition by hydrogen peroxide in Figure 5. Thus, traces of H_2O_2 trapped within the enzyme layer detected in the solution adjacent to the enzyme film inhibit the O_2 electroreduction reaction, while

the electrocatalytic current increases upon stirring. For thicker films the current difference between unstirred and stirred solutions is larger, which is consistent with the accumulation of peroxide and inhibition of the cathodic reduction of oxygen.

Many, but not all biofuel cells operate under stagnant conditions; therefore, the inhibition reported in the present work is very relevant to their performance. While the inhibition mechanism is not fully understood at present and is the matter of investigation, it is assumed that the release of peroxide from the trinuclear T2/T3 cluster and accumulation in the enzyme layer would interfere with the four-electron O_2 reduction mechanism proposed by Solomon^{5,54} since the addition of peroxide to the external solution also inhibits the reaction.

During the reviewing process one of the reviewers pointed out to a recent paper in press⁶⁰ where the production of peroxide by electroreduction of oxygen at the supporting carbon material is reported to cause deactivation of laccase. In the present work, however, we have demonstrated that peroxide is formed from enzymatic reduction of oxygen and that traces of peroxide trapped in the enzyme layer inhibit laccase, particularly under stagnant conditions. Furthermore, the inhibition of laccase is reversible, and the laccase activity is recovered upon removing the peroxide or stirring the electrolyte.

4. Conclusions

This paper presents new experimental evidence on O_2 biocathodes based on *Trametes trogii* laccase multilayers wired with an osmium complex under unstirred conditions: Peak and hysteresis in the polarization curves for O_2 reduction and abnormal shape in plots of the catalytic current vs O_2 concentration. These effects offset upon stirring the solution adjacent to the electrode with the RDE or with the intercalation of peroxidase layers in the self-assembled LbL construct. The experimental evidence presented here have been interpreted by the biocatalytic formation of peroxide from oxygen reduction and its accumulation within the enzyme film.

Hydrogen peroxide has been detected by SECM as a product of the biocatalyzed O_2 electroreduction by laccase mediated by Os (II). Control experiments have shown that peroxide is formed at potentials where O_2 cannot be reduced at the underlying Au surface or directly by Os (II) species. The yield of H_2O_2 at the SECM ultra-microelectrode tip follows the same trend and hysteresis as the redox-enzymatic O_2 reduction does, while inhibition of the enzyme by sodium azide stops the yield of peroxide.

In H_2O_2 -containing electrolyte inhibition of the O_2 catalytic current is observed, while addition of peroxide to air-saturated laccase solutions also results in inhibition of the enzyme activity measured by ABTS. To the best knowledge of the authors this is the first report of the inhibitory action of exogenous hydrogen peroxide on laccase.

All these findings have also been observed for *Trametes versicolor* laccase, indicating that they are a general feature of this enzyme from different organisms.

The new kinetic evidence presented in this paper is very relevant to the operation of most biofuel cells under stagnant conditions. The inhibition of laccase by hydrogen peroxide first

(60) Shleev, S.; Shumakovich, G.; Morazova, O.; Yaropolov, A. *Fuel Cells* **2010**, DOI: 10.1002/fuce.200900191.

reported here is of more general interest since laccase is an industrially relevant enzyme.

Acknowledgment. Financial support from ANPCyT Grant PICT 2006 1146, Universidad de Buenos Aires and CONICET is acknowledged. We thank Nestor J. Filieil for the purification of laccase. E.J.C. thanks Prof. P. N. Bartlett for very fruitful discussions.

Supporting Information Available: Purification and characterization of laccase, quartz crystal microbalance, and further electrochemical evidence. This material is available free of charge via the Internet at <http://pubs.acs.org>.

JA1020487